

# A concerted, alternating sites mechanism of ubiquinol oxidation by the dimeric cytochrome $bc_1$ complex

Bernard L. Trumpower\*

Department of Biochemistry, Dartmouth Medical School, Hanover, NH 03755-3844, USA

Received 12 March 2002; received in revised form 8 April 2002; accepted 8 April 2002

## Abstract

A refinement of the protonmotive Q cycle mechanism is proposed in which oxidation of ubiquinol is a concerted reaction and occurs by an alternating, half-of-the-sites mechanism. A concerted mechanism of ubiquinol oxidation is inferred from the finding that there is reciprocal control between the high potential and low potential redox components involved in ubiquinol oxidation. The potential of the Rieske iron–sulfur protein controls the rate of reduction of the *b* cytochromes, and the potential of the *b* cytochromes controls the rate of reduction of the Rieske protein and cytochrome  $c_1$ . A concerted mechanism of ubiquinol oxidation reconciles the findings that the ubiquinol–cytochrome *c* reductase kinetics of the  $bc_1$  complex include both a pH dependence and a dependence on Rieske iron–sulfur protein midpoint potential.

An alternating, half-of-the-sites mechanism for ubiquinol oxidation is inferred from the finding that some inhibitory analogs of ubiquinol that block ubiquinol oxidation by binding to the ubiquinol oxidation site in the  $bc_1$  complex inhibit the yeast enzyme with a stoichiometry of 0.5 per  $bc_1$  complex. One molecule of inhibitor is sufficient to fully inhibit the dimeric enzyme, and the binding is anti-cooperative, in that a second molecule of inhibitor binds with much lower affinity to a dimer in which an inhibitor molecule is already bound.

An alternating, half-of-the-sites mechanism implies that, at least under some conditions, only half of the sites in the dimeric enzyme are reactive at any one time. This provides a *raison d'être* for the dimeric structure of the enzyme, in that  $bc_1$  activity may be regulated and capable of switching between a half-of-the-sites active and a fully active enzyme.

© 2002 Elsevier Science B.V. All rights reserved.

**Keywords:** Cytochrome  $bc_1$  complex; Q cycle; Ubiquinol; Rieske iron–sulfur protein; Concerted mechanism

## 1. Introduction

Although the protonmotive Q cycle mechanism of the cytochrome  $bc_1$  complex is generally understood [1], the mechanism of ubiquinol oxidation at center P has not been fully elucidated. Ubiquinol oxidation is a divergent reaction in which electrons are transferred to the Rieske iron–sulfur protein and to cytochrome *b*. It is unclear whether ubiquinol is oxidized through a semiquinone intermediate in two sequential reactions, or whether ubiquinol is oxidized by the iron–sulfur protein and cytochrome  $b_L$  in a concerted reaction. There is no evidence of a semiquinone intermediate at center P. However, the predicted properties of such a semiquinone are such that it would not exist in detectable

concentrations, and thus, the absence of semiquinone cannot be taken as evidence for a concerted mechanism.

Crystal structures of the cytochrome  $bc_1$  complex suggest that movement of the iron–sulfur protein is necessary for electron transfer to cytochromes  $c_1$  and *b* [2]. However, both sequential and concerted electron transfer mechanisms can accommodate iron–sulfur protein movement. Similarly, mechanisms that propose occupancy of two ubiquinol molecules at center P [3,4] can be either sequential or concerted.

The crystal structures of the cytochrome  $bc_1$  complex also demonstrate that the enzyme is dimeric [2,5–7]. Oligomeric enzyme structures generally serve some function relevant to the enzyme mechanism. However, the Q cycle mechanism does not require a dimeric structure, and it is thus unclear what function is served by the  $bc_1$  dimer.

In this review, I propose that ubiquinol oxidation is a concerted reaction and that the reaction alternates between the two halves of the  $bc_1$  dimer. A concerted mechanism of

\* Tel.: +1-603-650-1621; fax: +1-603-650-1389.

E-mail address: Trumpower@Dartmouth.edu (B.L. Trumpower).

ubiquinol oxidation reconciles numerous experimental observations that otherwise seem contradictory and the half-of-the-sites activity allows for a novel form of regulation of  $bc_1$  activity that provides a *raison d'être* for the dimeric structure of the enzyme.

## 2. Results and discussion

### 2.1. A concerted, alternating sites mechanism of ubiquinol oxidation

The concerted oxidation of ubiquinol is outlined in reactions 1a–1c in the protonmotive Q cycle shown in Fig. 1. The concerted reaction begins when ubiquinol replaces the ionizable proton from the imidazole nitrogen of His-181, which is one of the ligands to the redox active iron of the Rieske cluster [8], to form a ubiquinol–imidazolate complex (reaction 1a). Formation of a ubiquinol–imidazolate complex in this manner circumvents prerequisite ionization of ubiquinol, which has a  $pK_a = 11.25$  [9], and makes the reaction rate independent of the  $pK_a$  of the quinol and dependent on the  $pK_a$  of the histidine imidazole group. Formation of the ubiquinol–imidazolate complex is responsible for the component of the bell-shaped activity vs. pH curves with attributed  $pK_a = 6.5–6.7$  [10] and 7.5 [11].

The ubiquinol–imidazolate complex is the electron donor for the iron–sulfur cluster and the  $b_L$  heme. This electron transfer does not occur unless the quinol–imidazolate complex forms a hydrogen bond to Glu-272 of cytochrome *b*, docked within electron transfer distance of the  $b_L$  heme (reaction 1b), so that electrons are transferred simultaneously from the quinol–imidazolate complex to the Rieske cluster and the  $b_L$  heme (reaction 1c).

A model of such a quinol–imidazolate–carboxylate complex was generated by manually docking ubiquinol in place of the stigmatellin residue in the stigmatellin-liganded yeast structure as shown in Fig. 2. In this model, one quinol hydroxyl group is hydrogen to the imidazole ring that is a ligand to the redox active iron of the Rieske cluster, while the other hydroxyl group is 10.5 Å from the porphyrin ring of heme  $b_L$ . The latter distance will be a determinant of the electron transfer rate, and some additional movement of the docked quinol–imidazolate complex toward the  $b_L$  heme is one possible source of the relatively high activation energy for quinol oxidation, as discussed below.

Binding of the ubiquinol only occurs when the iron–sulfur protein is proximal to cytochrome  $b_L$ , since formation of the ubiquinol–imidazolate complex (reaction 1a) is unfavorable unless it is docked to Glu-272 of cytochrome *b* (reaction 1b). If either cytochrome  $b_L$  or iron–sulfur protein is reduced, ubiquinol oxidation cannot occur, and ubiquinol cannot bind. As cytochrome *b* is reduced, the hydrogen bond to Glu-272 is broken, allowing the protonated Glu-272 to rotate toward the aqueous interface of center P as proposed by Crofts et al. [12], while ubiquinone

dissociates (reaction 1c) as the productive complex is dissipated. The reduced iron–sulfur protein then moves toward cytochrome  $c_1$  and electron transfer to  $c_1$  ensues (reaction 2 in Fig. 1). In this manner, association of ubiquinol and dissociation of ubiquinone are linked to the movement of the iron–sulfur protein between cytochromes *b* and  $c_1$ .

### 2.2. Evidence for a concerted mechanism of ubiquinol oxidation

The divergent oxidation of ubiquinol at center P results in the transient reduction of two redox centers, the iron–sulfur cluster of the Rieske protein and the  $b_L$  heme of cytochrome *b*, which differ in midpoint potential by  $\sim 300$  mV. The significance of this potential increment can be appreciated from the thermodynamic profile of the Q cycle shown in Fig. 3. Other reactions in the Q cycle, electron transfer from  $b_L$  to  $b_H$ , reduction of ubiquinone to ubisemiquinone, and reduction of ubisemiquinone to ubiquinol involve only modest changes in potential.

Whereas electron transfer from ubiquinol to the Rieske cluster is significantly exergonic, electron transfer from ubiquinol to the  $b_L$  heme is usually somewhat less endergonic. Ubiquinol oxidation is a concerted reaction in which the two electron transfers are mechanistically coincident and thermodynamically linked. The energy from reduction of the iron–sulfur cluster is used to drive reduction of the  $b_L$  heme. The *net* free energy change of these two electron transfer contributes the  $\Delta G$  term that is used, along with the distance to the  $b_L$  heme, to calculate rates of electron transfer by tunneling in the concerted mechanism.

We have shown that there is reciprocal control between the high potential and low potential redox components involved in ubiquinol oxidation at center P [16]. The potential of the Rieske iron–sulfur protein controls the rate of reduction of the *b* cytochromes, and the potential of the *b* cytochromes control the rate of reduction of the Rieske protein and cytochrome  $c_1$ . The relationship between iron–sulfur protein midpoint potential and rate of cytochrome *b* reduction is shown in Fig. 4a. The iron–sulfur protein midpoint potential was lowered by introducing mutations into the Rieske protein that eliminate hydrogen bonds to the iron–sulfur cluster [17]. A high resolution crystal structure of the peripheral domain of the Rieske iron–sulfur protein showed that the hydroxyl group of Ser-183 is hydrogen-bonded to S-1 of the [2Fe–2S] cluster and the hydroxyl group of Tyr-185 is hydrogen-bonded to the  $S_\gamma$  of Cys-159, a ligand of Fe-1 [8]. We reasoned that these hydrogen bonds delocalize electrons out of the reduced iron–sulfur cluster, and that if they were eliminated, the midpoint potential of the cluster would decrease. Eliminating these two hydrogen bonds dropped the midpoint potential of the cluster by 180 mV [17].

In the experiment shown in Fig. 4a, the  $bc_1$  complex was reduced with menaquinol and antimycin was included to

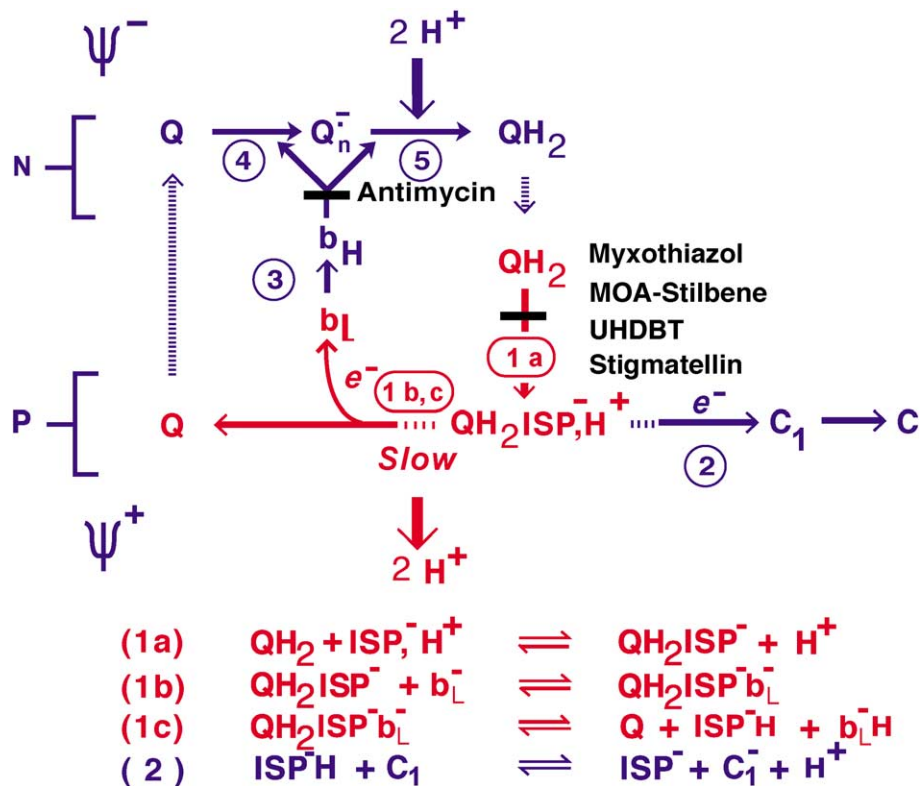


Fig. 1. The protonmotive Q cycle. Electron transfer reactions are numbered and circled. Dashed arrows designate movement of ubiquinol or ubiquinone between centers N and P and the quinone pool and movement of the iron–sulfur protein between cytochromes *b* and *c*<sub>1</sub>. Solid black bars indicate sites of inhibition by antimycin at center N, and by myxothiazol, MOA-stilbene, UHDBT, and stigmatellin at center P. Oxidation of ubiquinol at center P is depicted as a concerted reaction, consisting of three component reactions, 1a–1c, shown in red. In reaction 1a, ubiquinol replaces a proton of the imidazole nitrogen of His-181 on the Rieske iron–sulfur protein, which is a ligand to the redox active iron of the iron–sulfur cluster, to form a quinol–imidazolate complex. In reaction 1b, the quinol–imidazolate complex forms a hydrogen bond to Glu-272 of cytochrome *b*, docked within electron transfer distance from the *b*<sub>L</sub> heme. In reaction 1c, electrons are transferred simultaneously from the quinol–imidazolate–carboxylate complex to the iron of the Rieske cluster and the *b*<sub>L</sub> heme, resulting in dissociation of the complex and release of ubiquinol. The equilibria of reactions 1a and 1b lie toward the left while that of reaction 1c lies toward the right, provided that the Rieske cluster and the *b*<sub>L</sub> heme are oxidized. In reaction 2, the reduced Rieske cluster oscillates to within electron transfer distance of cytochrome *c*<sub>1</sub>, resulting in electron transfer from the iron–sulfur cluster to the *c*<sub>1</sub> heme. Two protons are released from center P when the Rieske cluster is oxidized by cytochrome *c*<sub>1</sub> and the protonated Glu-272 of cytochrome *b* dissociates from the electron transfer complex and moves toward the aqueous interface as suggested by Crofts et al. [12]. In reaction 3, an electron is transferred from the *b*<sub>L</sub> to *b*<sub>H</sub> heme, which in turn reduces ubiquinone to ubiquinol (reaction 4). Following oxidation of a second ubiquinol at center P and reduction of the *b* cytochromes, the *b*<sub>H</sub> heme reduces ubiquinol to ubiquinol (reaction 5), accompanied by uptake of two protons at center N.

block reduction of cytochrome *b* through center N. This is essential to insure that cytochrome *b* will be reduced through center P. Under these conditions, the second order rate constant for pre-steady state reduction of cytochrome *b* decreases by approximately two orders of magnitude as the midpoint potential of the Rieske cluster decreases by 180 mV. This decline in rate through center P accounts for the decline in ubiquinol–cytochrome *c* reductase activity resulting from the decreased midpoint potential of the Rieske cluster [17]. The decline in rate of *b* reduction also confirms the kinetic relationship between heme *b*<sub>L</sub> and the Rieske cluster implicit in the thermodynamic profile of the Q cycle shown in Fig. 3.

The potential of the *b* cytochromes also controls the rate of reduction of the Rieske protein and cytochrome *c*<sub>1</sub>. This is illustrated by the results of the experiment shown in Fig. 4b. In this experiment, we examined the effects of antimycin or ubiquinol residing at center N on the pre-steady state

rate of reduction of cytochrome *c*<sub>1</sub> by menaquinol. The rates of cytochrome *c*<sub>1</sub> reduction were measured at multiple menaquinol concentrations and second order rate constants were calculated from the slopes of the curves in Fig. 4b. With *bc*<sub>1</sub> complex in which endogenous ubiquinone is present, the second order rate constant for cytochrome *c*<sub>1</sub> reduction declined ~ 4.5-fold, from  $6.9 \times 10^5$  to  $1.55 \times 10^5$  M<sup>-1</sup> s<sup>-1</sup>, as the concentration of menaquinol increased. The reason for this decline in rate constant with increasing menaquinol concentrations is discussed below. When antimycin was added, the rate constant decreased by 10-fold to  $6.6 \times 10^4$  M<sup>-1</sup> s<sup>-1</sup>. With the *bc*<sub>1</sub> complex from the  $\Delta\text{coq}2$  mutant, the second order rate constant for *c*<sub>1</sub> reduction was  $1.1 \times 10^5$  M<sup>-1</sup> s<sup>-1</sup>, and the rate constant did not change when antimycin was added. From these rate constants, it is clear that in the presence of endogenous ubiquinone, antimycin slows the rate of *c*<sub>1</sub> reduction, but in the absence of endogenous ubiquinone, antimycin has no effect. These

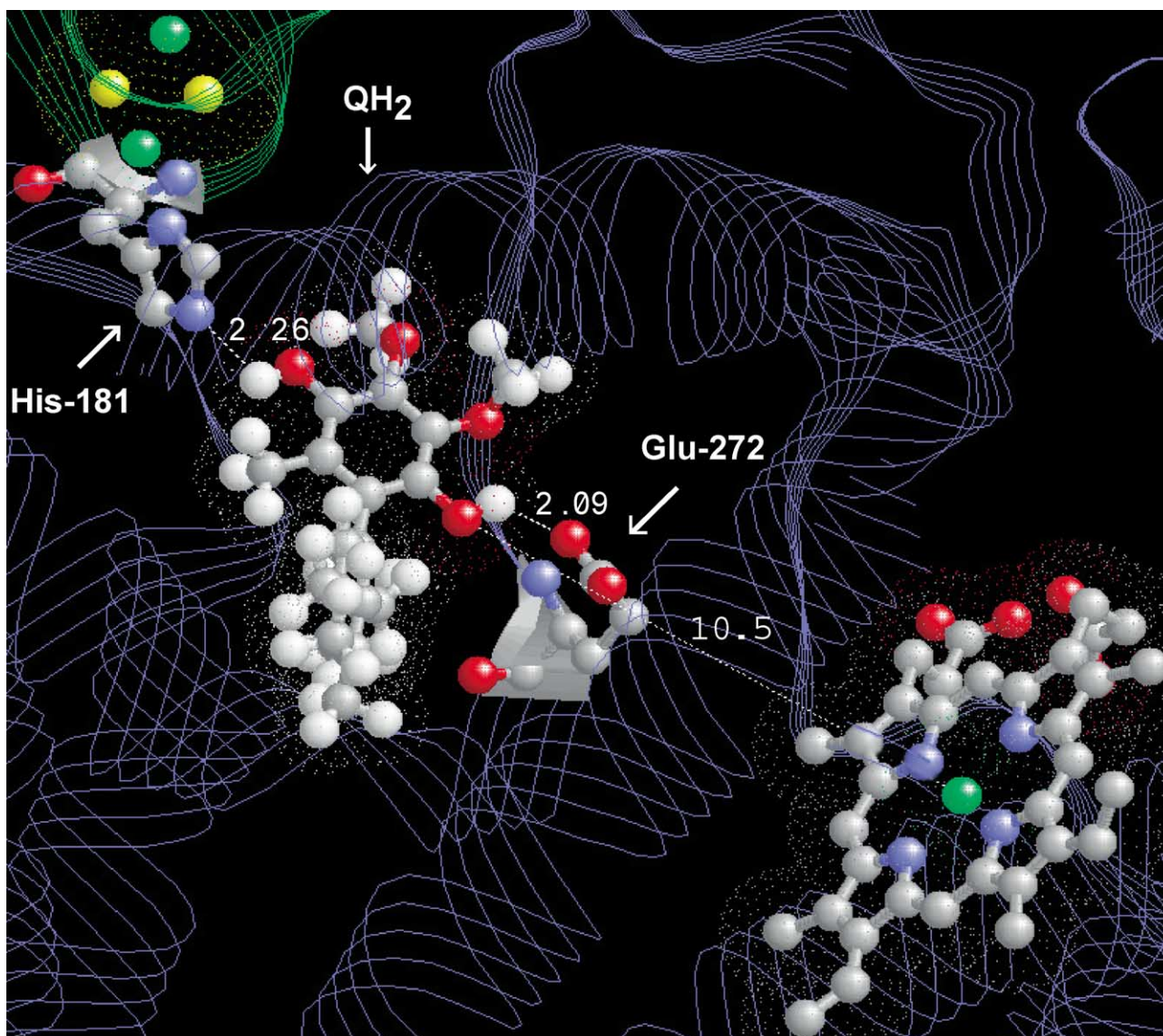


Fig. 2. Ubiquinol hydrogen bonded to His-181 of the Rieske iron–sulfur protein and Glu-272 of cytochrome *b* in the yeast cytochrome *bc*<sub>1</sub> complex. The view is from the membrane interior, looking toward center P. Ubiquinol, the *b*<sub>L</sub> heme, and His-181 of the Rieske protein and Glu-272 of cytochrome *b* are shown as ball and stick models, with nitrogen atoms colored blue, oxygen atoms colored red, and carbon atoms colored gray. Portions of the Rieske protein and cytochrome *b* are represented as green and blue strands, respectively. The iron–sulfur cluster is at the upper left, with iron and sulfur atoms colored green and yellow. The *b*<sub>L</sub> heme is at the lower right, with the iron atom colored green. Dashed white lines indicate the hydrogen bonds between the quinol hydroxyl groups and the imidazole nitrogen of His-181 of the Rieske protein and the carboxyl oxygen of Glu-272 of cytochrome *b*, and the distances are indicated in Angstroms. The distance between the quinol oxygen and the *b*<sub>L</sub> heme is similarly indicated. Ubiquinol containing two isoprenyl groups in the side chain was built with MacSpartan Pro (Wavefunction, Inc.) and docked manually into the Q<sub>p</sub> site by replacing stigmatellin in the coordinates for the stigmatellin-liganded yeast enzyme [7] as described elsewhere for the chicken heart enzyme [12].

results also indicate that absence of endogenous ubiquinone mimics the effect of antimycin on pre-steady state reduction of *c*<sub>1</sub> by menaquinol when ubiquinone is present.

In these pre-steady state experiments, two molecules of menaquinol are sequentially oxidized at center P. During the first turnover, the iron–sulfur protein and cytochrome *b*<sub>L</sub> are reduced (reactions 1a–1c in Fig. 1). The iron–sulfur protein will remain predominately reduced since its potential is higher than that of cytochrome *c*<sub>1</sub>. Cytochrome *b*<sub>L</sub> immediately reduces cytochrome *b*<sub>H</sub>, which then reduces ubiqui-

none to ubisemiquinone at center N (reactions 3 and 4 in Fig. 1). The second turnover at center P is dependent upon the redox state of cytochrome *b*<sub>L</sub> and the iron–sulfur protein, and will occur only when both are oxidized.

When ubiquinone is absent or when antimycin occupies center N, the electron introduced during the first turnover will remain in cytochrome *b* and equilibrate between the *b*<sub>H</sub> and *b*<sub>L</sub> hemes. Thus, absence of ubiquinone or the presence of antimycin has the effect of lowering the potential of cytochrome *b* after the first turnover in a pre-steady state

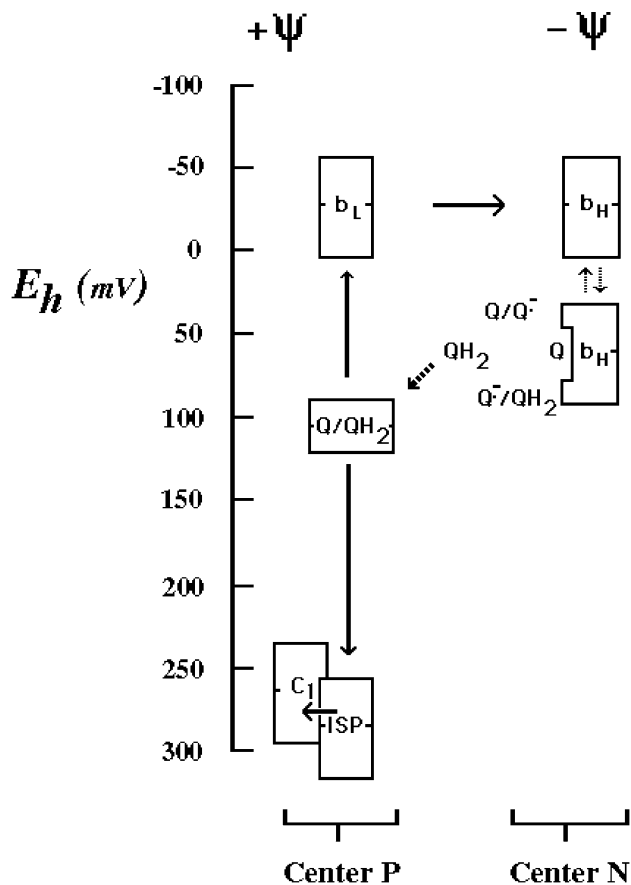


Fig. 3. Thermodynamic profile of the Q cycle. The figure depicts the thermodynamic relationship between the redox components of the yeast cytochrome  $bc_1$  complex at pH 7, with some uncertainties and exceptions as noted below. The redox groups are arranged vertically according to their oxidation–reduction potentials and horizontally according to their disposition across the inner mitochondrial membrane. The open boxes delineate the approximate range of potentials spanned by the redox components as their oxidation–reduction status varies in response to changes in rates of electron transfer through the  $bc_1$  complex. The centers of the boxes are positioned vertically at the midpoint potentials of the redox centers. The midpoint potentials of the cytochromes and iron–sulfur protein are those measured at room temperature for purified yeast  $bc_1$  complex at pH 7.0 [13]. Cytochrome  $b_H$  is assumed to be a mixture of two potentiometric species, as in the bovine enzyme [14]. Ubiquinone bound proximal to the  $b_H$  heme raises the potential of a portion of the  $b_H$  heme to +60 mV. Reduction of the quinone to quinol lowers the potential of the  $b_H$  heme to –30 mV. The potential of the ubiquinone pool is taken as 110 mV, the value measured at liquid nitrogen temperature [13]. The potentials of the ubisemiquinone couples at center N are estimates that assume the potential of the invisible, anti-ferromagnetically coupled semiquinone [15] is within range of the high potential form of cytochrome  $b_H$  since this heme group reduces both ubisemiquinone couples at center N.

experiment. The results in Fig. 4b show that when antimycin is present or when ubiquinone is absent, the rate of cytochrome  $c_1$  reduction is dramatically slowed. Furthermore, antimycin had no additional slowing effect when ubiquinone is absent. These results show that lowering the potential of cytochrome  $b$  by equilibration of an electron between cytochromes  $b_H$  and  $b_L$  slows reduction of the Rieske protein and cytochrome  $c_1$ .

This same effect accounts for the decline in second order rate constant for  $c_1$  reduction in the  $bc_1$  complex in the absence of antimycin as the concentration of menaquinol increases. As the menaquinol concentration increases, the endogenous ubiquinone becomes partly reduced, resulting in equilibration of an electron between ubiquinone and

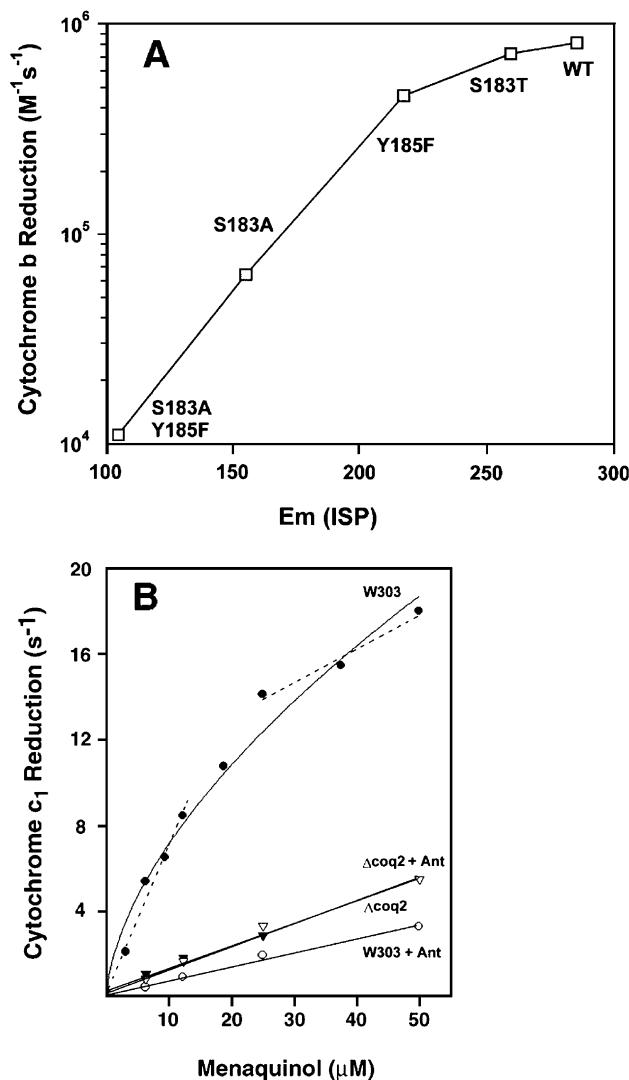


Fig. 4. Reciprocal control between the high and low potential redox components involved in ubiquinol oxidation. Panel A shows the effect of Rieske iron–sulfur protein midpoint potential on the second order rate constants for cytochrome  $b$  reduction, which were measured in the presence of antimycin to insure that the reaction proceeds through center P. The second order rate constants for cytochrome  $b$  reduction are plotted as a function of iron–sulfur protein midpoint potential for the  $bc_1$  complexes with the indicated iron–sulfur protein mutations. Panel B shows rates of cytochrome  $c_1$  reduction in wild-type and ubiquinol-deficient cytochrome  $bc_1$  complex in the absence or presence of antimycin. The rates of cytochrome  $c_1$  reduction are plotted as a function of menaquinol concentration for cytochrome  $bc_1$  complex from wild-type yeast ( $W303$ ) or  $bc_1$  complex from a yeast mutant lacking ubiquinone ( $\Delta coq2$ ), in the presence or absence of antimycin ( $Ant$ ). Dashed lines indicate the slopes that were used to calculate two second order rate constants for the  $bc_1$  complex from the wild-type yeast ( $W303$ ).

cytochrome *b*. Consequently, as the concentration of menaquinol increases, the second order rate constant for  $c_1$  reduction in the  $bc_1$  complex in which endogenous ubiquinone is present approaches the rate constants seen in the presence of antimycin or absence of ubiquinone.

We have interpreted this reciprocal control as evidence that oxidation of ubiquinol is a concerted reaction. However, this can also be explained by a sequential mechanism in which reduction of the iron–sulfur cluster by ubiquinol and reduction of the cytochrome  $b_L$  heme are thermodynamically linked in an obligatory manner. In such a mechanism, reduction of the Rieske iron–sulfur protein cannot proceed unless the ubisemiquinone intermediate is oxidized by reduction of cytochrome *b* [18–20]. The distinction between concerted and sequentially linked mechanisms and evidence that favors a concerted mechanism are discussed below.

### 2.3. Evidence for half-of-the-sites reactivity

There are numerous inhibitors of the  $bc_1$  complex that are thought to mimic ubiquinol or ubisemiquinone and that inhibit the enzyme by binding to the ubiquinol oxidase site at center P. We have found that some of these inhibitors act with a stoichiometry of 0.5 per cytochrome  $c_1$ , indicating that one molecule of inhibitor is sufficient to fully inhibit the dimeric enzyme [21].

We used two experimental approaches to demonstrate half-of-the-sites activity of center P inhibitors. In one, we determined the titer for inhibition of enzyme activity, and in the other, we determined the titer of inhibitor binding by measuring a shift in the cytochrome *b* optical spectrum that is dependent on binding of the inhibitor. The titration curves in Fig. 5 illustrate these two types of experiments. The data in Fig. 5a show the inhibition of yeast  $bc_1$  complex activity with stigmatellin in an assay that measures pre-steady state reduction of cytochrome *b* by menaquinol through center P. As can be seen from the titration curve, 0.5 equivalents of stigmatellin per  $bc_1$  complex fully inhibit this reaction. We also determined the titer for inhibition of oxidant-induced reduction of cytochrome *b* and ubiquinol–cytochrome *c* reductase activity, and found that 0.5 equivalents of stigmatellin per  $bc_1$  complex fully inhibit these activities also [21].

The data in Fig. 5b show the shift in the optical spectrum of cytochrome *b* that results from binding of MOA-stilbene, a methoxyacrylate inhibitor that also binds to center P. As can be seen from the titration curve, there is a progressive increase in the magnitude of the absorbance increment until 0.5 equivalents of MOA-stilbene per  $bc_1$  complex are bound. As additional MOA-stilbene is added, there is a more gradual increase in the absorbance increment. This biphasic titration curve is attributable to high affinity binding of MOA-stilbene to one half of the dimer and binding of a second molecule of the inhibitor to the second half of the dimer with much lower affinity. From a titration curve for inhibition of cytochrome *c* reductase activity, we estimated

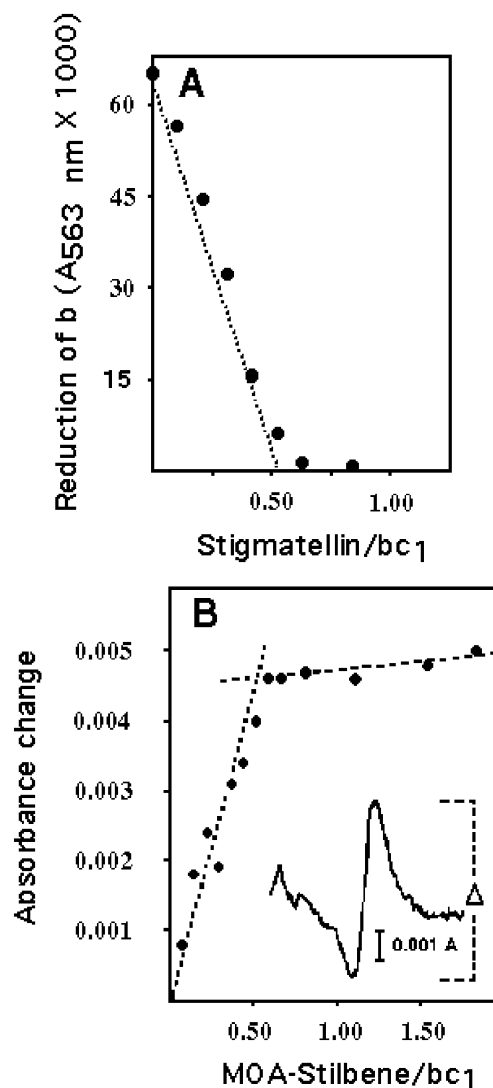


Fig. 5. Anti-cooperative binding to half of the sites in the dimeric cytochrome  $bc_1$  complex by inhibitory ubiquinol analogues. Panel A shows the titration of yeast  $bc_1$  complex with stigmatellin in an assay that measures pre-steady state reduction of cytochrome *b* by menaquinol through center P. The  $bc_1$  complex was pre-mixed with 2 equivalents of antimycin to block reduction of *b* through center N and then titrated with varying amounts of stigmatellin as indicated. Pre-steady state reduction of cytochrome *b* was followed at 563 nm in the stopped flow spectrophotometer and is plotted against the ratio of stigmatellin per  $bc_1$  complex. The dashed lines show the linear fitting to 0.5 equivalent of inhibitor per  $bc_1$  complex. Panel B shows a titration of the red shift in the cytochrome *b* spectrum that is induced by binding of MOA-stilbene. Purified cytochrome  $bc_1$  complex from the wild-type yeast strain, W303a, was reduced with dithionite and titrated with increasing amounts of MOA-stilbene. The inset shows the difference spectrum resulting from the red shift in the optical spectrum of the reduced *b* upon binding of MOA-stilbene and the method used to measure the absorbance increment at 568–560 nm due to the red shift.

$K_i = 2.5$ – $5.0$  nM for the high affinity binding site for MOA-stilbene, and from the titration of the shift in the cytochrome *b* optical spectrum, we estimated  $K_d = 1.5$ – $2.5$   $\mu$ M for the low affinity site [21].

The titration curves for inhibition of cytochrome *c* reductase activities and pre-steady state reduction of cytochrome *b* indicate that one molecule of stigmatellin or MOA-stilbene is sufficient to fully inhibit the dimeric enzyme. In addition, the binding site of these two inhibitors is anti-cooperative, in that a second molecule of inhibitor binds with much lower affinity to a dimer in which an inhibitor is already bound. As discussed above, we estimated that binding of inhibitor to one site in the dimer raised the  $K_d$  for binding at the second site approximately three orders of magnitude [21].

We have proposed that ubiquinol binding is likewise anti-cooperative, and that ubiquinol binding in one monomer raises the  $K_d$  for ubiquinol binding in the other monomer [21]. Consequently, only half of the  $bc_1$  dimer is active at any one time, and ubiquinol oxidation alternates between the two halves of the dimer. Elsewhere we have discussed several reports in the literature that indicate the  $bc_1$  complex exhibits half-of-the-sites reactivity towards ubiquinol or inhibitory analogs [21]. To this evidence, we would add that a crystal structure of the yeast  $bc_1$  complex co-crystallized with cytochrome *c* shows only one molecule of cytochrome *c* bound to the dimeric enzyme, and ubiquinone is present in only half of the dimer [22].

Anti-cooperative binding of ubiquinol and inhibitory structural analogues requires that a structural change must be transmitted from the binding site in one monomer to the binding site in the other. If ubiquinol oxidation is a concerted reaction as proposed here, ubiquinol must bridge a nitrogen of the imidazole ring of His-181 on the Rieske protein and the carboxyl oxygen on Glu-272 of cytochrome *b* as shown in Fig. 2. In such a mechanism, it is easy to envision how a subtle change in the distance or relative orientation of these two residues could significantly change the affinity for ubiquinol or structural analogues. The Rieske iron–sulfur protein spans the  $bc_1$  dimer, with its transmembrane helix anchored in one monomer and its peripheral domain containing the iron–sulfur cluster extending into the other dimer [2,5–7]. We have suggested that van der Waals interactions between the Rieske protein and cytochrome *b* may transmit a structural change between the ubiquinol binding sites in the two monomers [21]. Experiments are in progress to test this possibility.

A mechanism in which only one half of the dimer is active allows for the possibility that, under some conditions, both halves of the dimer are active and that the activity of the  $bc_1$  complex may be regulated by switching between a half-of-the-sites active and a fully active enzyme. This would have to involve a conformational change in the enzyme that disrupts communication between the two monomers. One can only speculate as to what types of signals might bring about such a switch in the enzyme. It is also possible that the  $bc_1$  dimer functions with two different affinities for substrate, and that the second half of the dimer is only active when the concentration of ubiquinol is high, but kinetic evidence for this has not been seen.

#### 2.4. Comparison to alternative mechanism

An alternative to the concerted mechanism is one consisting of two sequential reactions in which reduction of the iron–sulfur cluster by ubiquinol and reduction of the cytochrome  $b_L$  heme are thermodynamically linked in an obligatory manner. In the “proton-gated affinity change” mechanism, stabilization of ubisemiquinone by anti-ferromagnetic coupling to the reduced iron–sulfur protein raises the potential of the iron–sulfur cluster such that the cluster cannot be oxidized by cytochrome  $c_1$  until the semiquinone is oxidized [18]. In another sequentially coupled mechanism, it has been proposed that the potential of the ubiquinol/ubisemiquinone couple at center P is more positive than that of the iron–sulfur cluster and that oxidation of the semiquinone is required to lower the potential of the couple [19,20]. The common feature of these mechanisms is that there is a distinct ubisemiquinone intermediate, although undetectable, and the semiquinone must be oxidized in order to allow a thermodynamically linked reaction to occur.

In a concerted mechanism, there is no semiquinone intermediate. According to this view, a semiquinone at center P only exists as an aberrant by-product, resulting from interruption of the concerted oxidation. This in turn may lead to formation of superoxide anion, or its protonated adduct, if the semiquinone reacts with oxygen. Formation of superoxide anion reflects the “error rate” at which the concerted reaction is disrupted.

Ubiquinol–cytochrome *c* reductase activity of the  $bc_1$  complex is pH-dependent, exhibiting a bell-shaped curve of activity vs. pH, with a maximum at pH 7.5–8.0 [10,11]. Brandt and Okum [10] were the first to suggest that this bell-shaped curve reflected opposing enhancement and retardation of catalysis and interpreted the curve as resulting from ionization of two functional groups with estimated  $pK_a=6.5-6.7$  and  $pK_a=9.1$ . They attributed the rate enhancement at low pH to dissociation of a proton from a proton acceptor group in the pathway of ubiquinol oxidation, but did not identify the group. They attributed the decline in activity at high pH to ionization of the imidazole group of one of the histidine ligands to the iron–sulfur cluster and a lowering of the midpoint potential of the Rieske iron–sulfur cluster due to the increased negative charge.

Covian and Moreno-Sanchez [11] have shown that the bell-shaped pH vs. activity curve can be better fit by assuming three protonatable groups with  $pK_a=5.2, 7.5,$  and  $9.2$ . They proposed that these are the carboxyl group of Glu-272 on cytochrome *b*, the imidazole nitrogen on His-181 of the Rieske protein, and the imidazole nitrogen on His-161 of the Rieske protein, respectively. Modeling of the bell-shaped pH vs. activity curve with three protonatable groups in this manner better fits the  $pK_a$  of His-181 deduced from the pH dependence of the Rieske midpoint potential [23] and agrees with the crystallographic structure implicating Glu-272 of cytochrome *b* in the catalytic cycle [12].

Contributions to the catalytic rate from these three protonatable groups is predicted from the concerted mechanism discussed above, since formation of the productive electron transfer complex requires ionization of both the Glu-272 ( $pK_a=5.2$ ) and the His-181 ( $pK_a=7.5$ ). The concerted mechanism also predicts a significant rate contribution from the Rieske midpoint potential, which would account for the declining rate associated with ionization of the His-161 imidazole group ( $pK_a=9.1$ ).

The activation energy for ubiquinol oxidation is 35–45 kJ/mol at ambient temperatures [10,24]. Hong et al. [24] have shown that the activation barrier is not formation of the ubiquinol–imidazolate complex or movement of the Rieske protein between cytochromes *b* and *c*<sub>1</sub>, and that the barrier occurs after formation of the ubiquinol–imidazolate complex. With these constraints, there remain two possible sources of the high activation energy. One possible source of the activation barrier is movement of the quinol–imidazolate complex closer to the *b*<sub>L</sub> heme after docking to Glu-272 of cytochrome *b* (reaction 1b in Fig. 1). This would shorten the 10.5-Å distance from the quinol oxygen to the *b*<sub>L</sub> heme (Fig. 2) prior to the electron transfer (reaction 1c in Fig. 1) and might be necessary if the  $\Delta G$  increment between the two electron transfers of the concerted reaction becomes small or positive. A second possible source of the activation barrier is movement of the Glu-272 of cytochrome *b* to or from the aqueous interface. Both of these alternatives involve a protein structural change and either could have a relatively large activation energy, although movement of the glutamate anion from the surface to the protein interior seems the more likely energy-requiring step.

From the preceding discussion, it should be clear that there are multiple kinetic and thermodynamic parameters that contribute to the ubiquinol oxidation rate. These include a three-component pH dependence [11], a relatively high activation energy [10,24], reciprocal control on rates of reduction between the *b*<sub>L</sub> heme and the Rieske cluster [16], and a  $2.5 \times /60$  mV dependence of rate on potential increment between the Rieske cluster and ubiquinol [17]. Although a sequential or a concerted mechanism can accommodate any one of these parameters equally well, it is hard to reconcile all of them with a sequential mechanism in which these parameters are distributed across segregated steps. However, all of these are incorporated into a single step in the concerted mechanism (reactions 1a–1c in Fig. 1).

## Acknowledgements

I wish to thank Dr. Ed Berry for modeling ubiquinol into the yeast crystal structure as shown in Fig. 2. This research was supported by NIH grant GM 20379.

## References

- [1] P. Mitchell, *J. Theor. Biol.* 62 (1976) 327–367.
- [2] Z.L. Zhang, L.S. Huang, V.M. Shulmeister, Y.I. Chi, K.K. Kim, L.W. Hung, A.R. Crofts, E.A. Berry, S.H. Kim, *Nature* 392 (1998) 677–684.
- [3] H.G. Ding, D.E. Robertson, F. Daldal, P.L. Dutton, *Biochemistry* 31 (1992) 3144–3158.
- [4] U. Brandt, *Biochim. Biophys. Acta* 1275 (1996) 41–46.
- [5] D. Xia, C.A. Yu, H. Kim, J.Z. Xian, A.M. Kachurin, L. Zhang, L. Yu, J. Deisenhofer, *Science* 277 (1997) 60–66.
- [6] S. Iwata, J.W. Lee, K. Okada, J.K. Lee, M. Iwata, B. Rasmussen, T.A. Link, S. Ramaswamy, B.K. Jap, *Science* 281 (1998) 64–71.
- [7] C. Hunte, J. Koepke, C. Lange, T. Rossmannith, H. Michel, *Struct. Fold. Des.* 8 (2000) 669–684.
- [8] S. Iwata, M. Saynowits, T.A. Link, H. Michel, *Structure* 4 (1996) 567–579.
- [9] P.R. Rich, *Biochim. Biophys. Acta* 768 (1984) 53–79.
- [10] U. Brandt, J.G. Okum, *Biochemistry* 36 (1997) 11234–11240.
- [11] R. Covian, R. Moreno-Sanchez, *Eur. J. Biochem.* 268 (2001) 5783–5790.
- [12] A.R. Crofts, S. Hong, N. Ugulava, B. Barquera, R. Gennis, M. Guergova-Kuras, E. Berry, *Proc. Natl. Acad. Sci. U. S. A.* 96 (1999) 10021–10026.
- [13] A.L. T'sai, G. Palmer, *Biochim. Biophys. Acta* 722 (1983) 349–363.
- [14] J.C. Salerno, Y. Xu, M.P. Osgood, C.H. Kim, T.E. King, *J. Biol. Chem.* 264 (1989) 15398–15403.
- [15] F.F. De la Rosa, G. Palmer, *FEBS Lett.* 163 (1983) 140–143.
- [16] C.H. Snyder, E.B. Gutierrez-Cirlos, B.L. Trumpower, *J. Biol. Chem.* 275 (2000) 13535–13541.
- [17] E. Denke, T. Merbitz-Zahradnik, O.M. Hatzfeld, C.H. Snyder, T.A. Link, B.L. Trumpower, *J. Biol. Chem.* 273 (1998) 9085–9093.
- [18] T.A. Link, *FEBS Lett.* 412 (1997) 257–264.
- [19] S. Jünemann, P. Heathcote, P.R. Rich, *J. Biol. Chem.* 273 (1998) 21603–21607.
- [20] A.R. Crofts, B. Barquera, R.B. Gennis, R. Kuras, M. Guergova Kuras, E.A. Berry, *Biochemistry* 38 (1999) 15807–15826.
- [21] E.B. Gutierrez-Cirlos, B.L. Trumpower, *J. Biol. Chem.* 277 (2002) 1195–1202.
- [22] C. Lange, C. Hunte, *Proc. Natl. Acad. Sci. U. S. A.* 99 (2002) 2800–2805.
- [23] T.A. Link, W.R. Hagen, A.J. Pierik, C. Assmann, G. von Jagow, *Eur. J. Biochem.* 208 (1992) 685–691.
- [24] S. Hong, N. Ugulava, M. Guergova-Kuras, A.R. Crofts, *J. Biol. Chem.* 274 (1999) 33931–33944.